Skeletal Radiol (2015) 44:1317–1325
DOI 10.1007/s00256-015-2158-9

SCIENTIFIC ARTICLE

Carbon fiber intramedullary nails reduce artifact in postoperative advanced imaging

Melissa N. Zimel[1] **· Sinchun Hwang**[2] **· Elyn R. Riedel**[3] **· John H. Healey**[1,4]

Received: 20 February 2015 / Revised: 17 April 2015 / Accepted: 20 April 2015 / Published online: 17 May 2015

Abstract

Objective This study assessed whether radiolucent carbon fiber reinforced-polyetheretherketone (CFR-PEEK) intramedullary nails decreased hardware artifact on magnetic resonance imaging (MRI) and computed tomography (CT) in vitro and in an oncologic patient population.

Materials and methods In vitro and clinical evaluations were done. A qualitative assessment of metal artifact was performed using CFR-PEEK and titanium nail MRI phantoms. Eight patients with a femoral or tibial prophylactic CFR-PEEK nail were retrospectively identified. All patients had postoperative surveillance imaging by MRI, CT, and were followed for a median 20 months (range, 12–28 months). CFR-PEEK images were compared to images from a comparative group of patients with titanium femoral intramedullary nails who had a postoperative MRI or CT. A musculoskeletal-trained radiologist graded visualization of the cortex, corticomedullary junction, and bone–muscle interface, on T1-weighted (T1W), STIR, and contrast-enhanced T1-weighted fat-saturated (T1W FS) sequences of both groups with a five-point scale, performing independent reviews 4 months apart. Statistical analysis used the Wilcoxon rank-sum test and a weighted kappa.

Results Substantially less MRI signal loss occurred in the CFR-PEEK phantom than in the titanium phantom simulation, particularly as the angle increased with respect to direction of the static magnetic field. CFR-PEEK nails had less MRI artifact than titanium nails on scored T1W, STIR, and contrast-enhanced T1W FS MRI sequences ($p \leq 0.03$). The mean weighted kappa was 0.64, showing excellent intraobserver reliability between readings.

Conclusions CFR-PEEK intramedullary nail fixation is a superior alternative to minimize implant artifact on MRI or CT imaging for patients requiring long bone fixation.

Keywords Carbon fiber · CFR-PEEK · Intramedullary nail · MRI artifact · CT artifact · Postoperative imaging · Oncology

Introduction

Patients with aggressive benign or malignant bone and soft tissue tumors often require wide surgical resection and local adjuvant treatment, placing them at high risk for pathologic fracture [1, 2]. Surgical adjuvants such as radiation therapy, cryosurgery, or argon beam coagulation not only increase the risk of fracture but also the rate of persistent bony nonunion [1, 3]. To prevent such complications after tumor resection, long bones are prophylactically fixed with an intramedullary nail or plate. However, MRI and CT artifact from traditional titanium or stainless-steel implants can obstruct necessary postoperative surveillance imaging and make it more challenging to detect recurrent disease [4].

Carbon fiber-reinforced polyetheretherketone (CFR-PEEK) orthopedic implants provide several advantages to

✉ John H. Healey
healeyj@mskcc.org

[1] Orthopaedic Surgery Service, Department of Surgery, Memorial Sloan Kettering Cancer Center, 1275 York Ave., New York, NY 10065, USA

[2] Department of Radiology, Memorial Sloan Kettering Cancer Center, 1275 York Ave., New York, NY 10065, USA

[3] Department of Epidemiology and Biostatistics, Memorial Sloan Kettering Cancer Center, 1275 York Ave., New York, NY 10065, USA

[4] Department of Orthopaedic Surgery, Weill Medical College of Cornell University, 1300 York Avenue, New York, NY 10021, USA

conventional orthopedic materials including an inert biochemical profile, a similar elastic modulus to bone, and mechanical toughness superior to other metal alloys [5]. Biomechanical testing of CFR-PEEK nails found the four-point bending strength, torsional stiffness, and bending fatigue to be comparable to commercially available titanium nails [5]. Given these findings, and the known inert biochemical and biologic properties of carbon fiber composite, the utilization of PEEK biomaterials in orthopedic trauma and spinal instrumentation has increased over recent decades [6].

The imaging characteristics of CFR-PEEK composite materials have been studied in spinal cage instrumentation and were found to be radiolucent regardless of the imaging modality used (e.g., radiography, CT, MRI), allowing for visualization of spinal fusion [5]. Radiographic analysis of CFR-PEEK composites confirmed superior radiolucency to other composites, allowing for complete cortical bone visualization [7]. Studies examining metal alloy implants found that titanium produces the least CT artifact, but still results in metallic streak artifact, limiting evaluation of immediate periprosthetic tissues [8, 9]. MRI studies detail methods of reducing intramedullary metal artifact, but are unable to eliminate distortion immediately adjacent to the implant [4, 10–12] in the surrounding marrow space, cortex, and bone–muscle interface.

The clinical and radiographic implications of carbon fiber intramedullary nails have yet to be described in current literature. Case reports and one patient series have studied the use of CFR-PEEK implants for fracture fixation, and highlighted radiographic advantages [13, 14]. The surgical indications for prophylactic long bone fixation in patients at high risk of fracture have been addressed in the literature [3], but did not address the effect on postoperative imaging. This study quantifies the artifact generated by CFR-PEEK intramedullary nails on both MRI phantom and on MRI and CT exams in an oncologic patient population, and describes their short-term clinical results.

Materials and methods

MRI phantom study Qualitative assessment of metal artifact from titanium and CFR-PEEK nails was performed using MRI phantoms to evaluate the extent of the artifact produced in relation to the position of the hardware along the static magnetic field (B_0). CFR-PEEK and titanium intramedullary nails were immersed in agarose gel and imaged separately at 1.5 T (Optima MR450w, GE Healthcare). Each phantom was scanned using an eight-channel cardiac coil in the axial plane in two positions. The nails were first placed on the table with their long axis parallel to the table and therefore parallel to the magnetic field B_0. After the images were obtained, the nails were positioned with their long axis oriented at a 35° angle oblique to the table. In each position, 2D fast spin echo (FSE) T1-weighted images were obtained with the following parameters; TR=500, TE=5.7 ms, four NEX with matrix 256×256 and bandwidth 62.5 kHz. STIR images were obtained using TR=2928, TE=53.4 ms with two NEX with matrix 256×192 and bandwidth of 62.5 kHz. Locations of signal loss and pile-up around the nails, as well as the distortion in the nail shapes, were evaluated with the AW Workstation (GE Healthcare, Milwaukee, WI, USA) using the same window settings for each sequence at the AW Workstation by a musculoskeletal fellowship-trained radiologist with 10 years of experience.

Study subjects With institutional review board-approved waiver of informed consent requirements, we retrospectively reviewed our institutional database and identified a series of eight adult oncology patients who underwent prophylactic tibial or femoral intramedullary fixation with a CarboFix (CarboFix Orthopedics Ltd., Herzeliya, Israel) CFR-PEEK nail from September 2012 to February 2014. There were four female and four male patients, with a mean age of 48 years (range, 30–89 years) at the time of surgery. All histologic diagnoses were reviewed and confirmed by a surgical musculoskeletal pathologist at our institution. Three patients had a soft tissue sarcoma resection [undifferentiated pleomorphic sarcoma (n=1); myxofibrosarcoma (n=2)] and adjuvant radiation therapy. Three patients had bony lesions [hemangioma of bone (n=1); adamantinoma (n=1); metastatic thyroid carcinoma (n=1)] requiring resection and local adjuvant therapy with cryosurgery or argon beam coagulation. The other two patients had pathologic bony lesions [fibrous dysplasia (n=1), sessile osteochondroma (n=1)] requiring stabilization for impending fracture. Patient demographics and diagnoses are outlined in Table 1. Prophylactic fixation was performed either at the time of tumor resection or in a delayed fashion as a secondary procedure after surgical margins were confirmed to be negative and sufficient wound healing after the initial procedure was achieved [15, 16].

CarboFix intramedullary nails were inserted in accordance with the steps outlined in the technical guide provided by the manufacturer. Femoral nails were placed in a retrograde fashion and all tibial nails were placed anterograde. Intramedullary reaming, nail insertion, and placement of titanium interlocking screws were performed under fluoroscopic guidance.

After the index procedure, patients were examined at routine intervals by an orthopedic oncologist to assess wound healing, range of motion, mobility, and pain. Patients with a malignant disease were imaged with an extremity MRI at standard intervals of 3 and 6 months per National Comprehensive Cancer Network (NCCN) guidelines [17]. CT imaging of the affected extremity was performed only in those patients with a contraindication to MRI. Patients with benign aggressive disease were imaged with radiographs, with advanced imaging ordered only if the patient exhibited pain or

Table 1 Summary of study population

Age (years)	Sex	Histologic diagnosis	Location	Nail type	Radiation therapy	Surgical adjuvant	MRI exams	CT exams
Carbon fiber nail patients								
47	F	Undifferentiated pleomorphic sarcoma	Vastus lateralis	Femoral	Yes	None	4	
39	F	Adamantinoma	Tibia	Tibial	No	Cryosurgery	4	
39	F	Sessile osteochondroma	Femur	Femoral	No	None		
35	M	Fibrous dysplasia with impending fracture	Tibia	Tibial	No	None		
64	M	High-grade myxofibrosarcoma	Vastus intermedius	Femoral	Yes	None	2	
30	F	Intramuscular hemangioma invading adjacent bone	Femur	Femoral	No	Argon beam		
89	M	Myxofibrosarcoma	Vastus intermedius	Femoral	Yes	None		2
44	M	Thyroid carcinoma cortical metastasis	Femur	Femoral	Yes	Cryosurgery	1	
Total							11	2
Titanium nail patients (controls)								
Age (years)	Sex	Histologic diagnosis	Location	Nail type	Radiation therapy	Surgical adjuvant	MRI exams	CT exams
71	M	Renal cell carcinoma metastasis	Femur	Femoral	Yes	None	2	
63	M	Non-small cell lung carcinoma cortical metastasis	Femur	Femoral	Yes	None	2	
41	M	Myxoid liposarcoma	Vastus intermedius	Femoral	Yes	None	3	
80	F	Dedifferentiated liposarcoma	Proximal-medial thigh	Femoral	Yes	None	2	
43	F	Thyroid carcinoma cortical metastasis	Femur	Femoral	Yes	None	1	
42	M	Myxofibrosarcoma	Vastus intermedius	Femoral	Yes	None	1	
65	F	Breast carcinoma metastasis	Femur	Femoral	Yes	None		1
Total							11	1

other concerning symptoms. All imaging studies were reviewed by a musculoskeletal radiologist to evaluate implant integrity and to look for evidence of recurrent disease.

For the purpose of comparative image analysis, a control group was retrospectively identified from our institutional database. Patients were included if they had a titanium femoral nail placed after resection of a soft tissue sarcoma or for an isolated bone metastasis, and a subsequent postoperative MRI or CT from 2011 to 2014. Patients with multifocal metastatic long bone disease requiring prophylactic nailing were not included given the diffuse abnormal characteristics of their marrow, cortex, and bone–muscle interface. The control group was comprised of seven patients, three females and four males, with a mean age 56 years (range, 41–71 years) at the time of surgery. Diagnoses included renal cell, breast, thyroid, and lung carcinoma (n=4), myxoid liposarcoma (n=1), dedifferentiated liposarcoma (n=1), and myxofibrosarcoma (n=1). Patient demographics are summarized in Table 1. All patients had adjuvant radiation therapy and required placement of an intramedullary nail for impending pathologic fracture.

All MRI scans were obtained with a 1.5-T system, and lower extremities were imaged with an eight-channel body coil or an extremity coil. Two-dimension fast spin-echo images were obtained with the following parameters: TR/TE, 400-683/7-15 ms for T1-weighted sequence (T1W) and contrast-enhanced T1-weighted fat-saturated; TR/TE (T1W FS), 4017–6400/37-67 ms for STIR with TI=150 ms; bandwidth, 62 kHz; number of signal acquired, 2–4; acquisition matrix, 256–320 (frequency) × 160–224 (phase); slice thickness, 7–10 mm; slice spacing, 0.5–2 mm.

Image analysis Image analysis was performed by the aforementioned musculoskeletal radiologist. All postoperative MRIs in both carbon-fiber and control groups were reviewed for a total of 22 studies, 11 in each group, with a mean of two studies per patient (Table 1). The radiologist graded visualization of the cortex, corticomedullary junction, and bone–muscle interface, anatomic areas immediately adjacent to the implant, on axial images of T1-weighted, STIR, and contrast-enhanced, T1-weighted fat-saturated sequences. Visualization was graded utilizing a five-point scoring system, with increasing scores corresponding to increasing percentages of anatomic area visualized, as follows: 1=<10, 2=10–30, 3=30–60, 4=60–90, and 5 = >90 %. The degree of fat saturation was also graded with a score of 1 (poor), 2 (fair), or 3 (good). The areas of interlocking screws were not included in this analysis. Scores within each sequence and anatomic region in carbon fiber patients were compared to scores in control (titanium) patients using the Wilcoxon rank-sum test.

Postoperative CT artifact was evaluated by analyzing studies performed on a single patient from each of the patient groups. Beam hardening artifact and visualization of anatomic areas adjacent to each implant were compared between implant types. This comparison was restricted to two patients given the limited number of lower extremity CTs performed for postoperative surveillance imaging. Given this small number of patients, the analysis was primarily descriptive.

Statistical analysis To evaluate intraobserver reliability of this scoring system, the same radiologist performed a second scoring of all MRI studies 4 months after the initial image analysis. The radiologist was blinded to prior scoring and interpretation. A weighted kappa was calculated to measure intraobserver agreement between the first and second readings of each anatomic area scored for each sequence. A kappa of 0.40–0.60 was considered to represent moderate agreement, 0.61–0.80 substantial agreement, and 0.81–0.99 near perfect agreement.

Results

Analysis of MRI phantoms Images acquired with both nails parallel to B_0 demonstrated that signal pile-up (high signal) and signal loss around the hardware was smaller and symmetrically distributed around the CFR-PEEK nail compared to the titanium nail in T1-weighted and STIR images (Figs. 1 and 2). The signal pile-up and signal loss was increased when the titanium nail was tilted 35° to the z-axis of B_0 of the scanner. The increase was substantial on both T1W and STIR sequences. In addition, the shape of the titanium nail was substantially distorted along the frequency encoding direction. In contrast, the CFR-PEEK nail did not demonstrate signal pile-up and signal loss when tilted 35° to the z-axis of B_0 (Figs. 3 and 4). This difference demonstrates the advantage of carbon fiber when imaging a patient with an implant that may not be parallel to the MRI table or $B_{0.}$

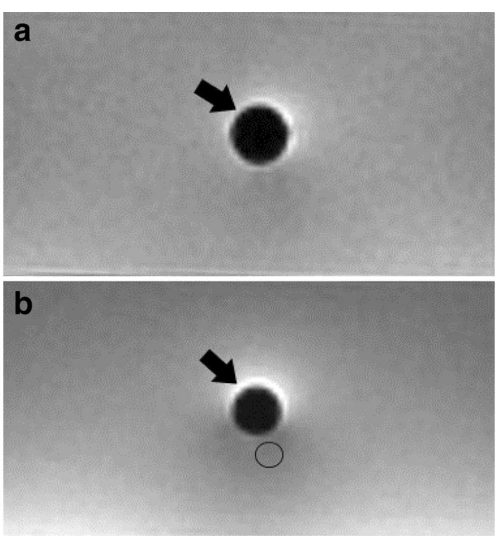

Fig. 1 T1-weighted sequence with nails positioned parallel to the *z*-axis of the magnetic field (B_0). The carbon fiber nail (**a**) shows a thin high signal rim of signal pile-up (*arrow*). The titanium nail (**b**) shows an asymmetric high signal rim of signal pile-up (*arrows*) and signal loss (*circled dark area*)

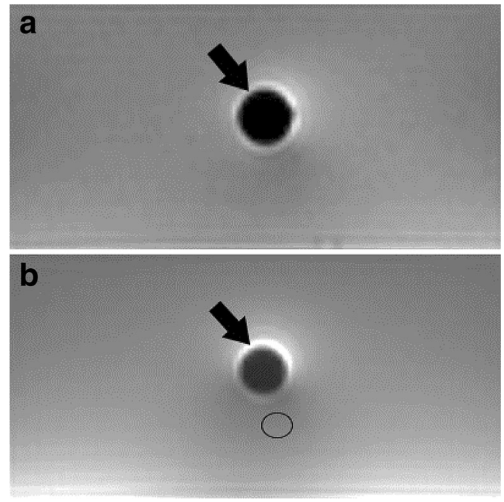

Fig. 2 STIR sequence with nails positioned parallel to z-axis. The carbon fiber nail (**a**) shows a thin high signal rim of signal pile-up (*arrow*). The titanium nail (**b**) shows an asymmetric high signal rim of signal pile-up (*arrows*) and signal loss (*circled dark area*)

Analysis of clinical MRI exams Wilcoxon rank-sum test analysis of graded axial MRI images found that CFR-PEEK nails have a statistically significant higher visualization score than the control group in all sequences and in all anatomic regions, with all p values ≤0.03. The complete MRI image analysis results are listed in Table 2. Mean scores from both readings of each analyzed sequence of both titanium control and CFR-PEEK nails are listed for each examined anatomic region. The mean cortex visualization score for CFR-PEEK on all sequences was 3.8, while only 2.8 for titanium nails, and this difference was statistically significant with p value from each sequence ≤0.02. Superior visualization of the corticomedullary junction in the CFR-PEEK group was observed with a mean score of 3.6 in all sequences compared to a mean score of 2.5 in the titanium group ($p \leq 0.02$). The mean muscle–bone interface score was 4.2 for CFR-PEEK, while only 3.0 for titanium; this difference was also statistically significant ($p \leq 0.03$). Thus, mean scores, utilizing our five-point scale, confirm a statistically significant superiority of the percentage of visualized cortex, corticomedullary junction, and muscle–bone interface on MRI images of carbon fiber nails secondary to decreased image artifact (Figs. 5 and 6).

Differences in fat suppression were also noted between both groups. The mean fat suppression score was 2.6 on STIR and contrast-enhanced T1W FS images in the carbon fiber

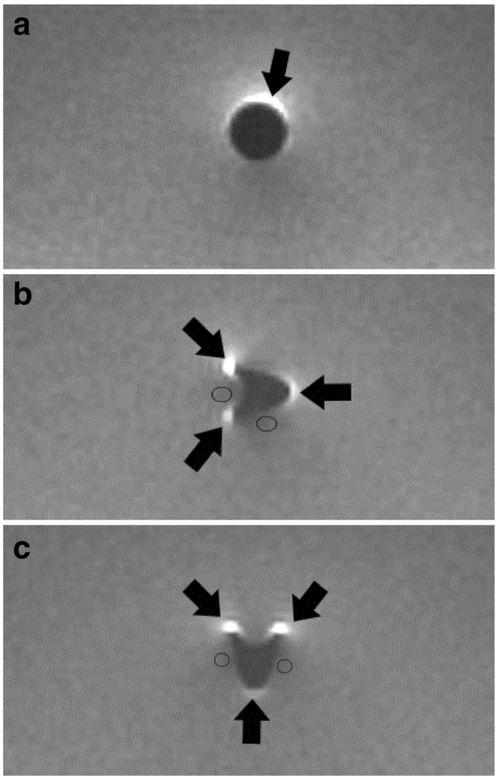

Fig. 3 T1-weighted sequence with nails positioned 35° tilted to *z*-axis of the magnetic field (B_0). The carbon fiber nail (**a**) shows an asymmetric thin high signal rim of signal pile-up (*arrow*). The titanium nail (**b**) shows substantial distortion of its shape and irregular signal pile-up (*arrows*) and signal loss (*circled areas*). When frequency encoding direction changed in a perpendicular direction, the distortion of its shape and direction of the signal pile-up (*arrows*) and signal loss (*circled dark areas*) also changed in the same direction (**c**)

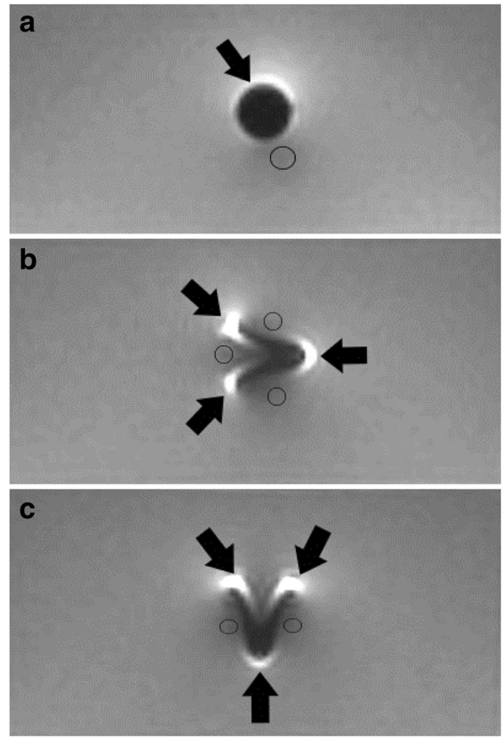

Fig. 4 STIR sequence with nails positioned 35° tilted to *z*-axis of the magnetic field (B_0). The carbon fiber nail (**a**) shows asymmetric thin rim of signal pile-up (*arrow*). The titanium nail (**b**) shows substantial distortion of its shape and irregular signal pile-up (*arrows*) and signal loss (*circles*). When the frequency encoding direction changes, the distortion of its shape and direction of the signal pile-up (*arrows*) and signal loss (*circles*) are also changed (**c**)

group and 1.8 on STIR and contrast-enhanced T1W FS images in the titanium group when averaged over all 11 studies (Figs. 5 and 6).

Analysis of CT exams Two CT studies of a patient with a carbon fiber femoral nail were available for review (Fig. 7). The beam-hardening artifact was substantially less compared to the patient with a titanium nail. The cortex, corticomedullary junction, and bone–muscle interface were nearly completely visualized while only partially visualized in the patient with a titanium nail secondary to streak artifact. Significant streak artifact obscures the tissues immediately adjacent to the titanium nail. This artifact is minimized in the patient with a carbon fiber implant.

During the postoperative follow-up period of the CFR-PEEK nail group (median, 20 months, range, 12–28 months), all patients were clinically and radiographically evaluated. No patients with a CFR-PEEK nail exhibited any objective or subjective evidence of surgical complications including, but not limited to, superficial or deep infection, painful or symptomatic hardware, or completion of an impending pathologic fracture. All patients were able to ambulate without an assistive device, and regained their preoperative knee range of motion within the early postoperative period. Of note, at the most recent follow-up, one patient in the CFR-PEEK group with metastatic thyroid carcinoma was found to have a new isolated cortical metastasis of the ipsilateral femur. This was observed on a follow-up MRI and was clearly visible adjacent to the nail, given the lack of implant artifact (Fig. 8). This MRI was not included in the image analysis given it occurred after the study analysis period. The remaining patients with CFR-PEEK nails exhibited no evidence of disease recurrence on follow-up surveillance imaging at their most recent follow-up.

Discussion

The primary goal of our study was to qualitatively and semi-quantitatively assess the differences between CFR-PEEK and titanium implant artifact seen on the MRI and CT surveillance images required to monitor for recurrent oncologic disease. These differences were confirmed with MRI phantoms of titanium and CFR-PEEK nails. Secondarily, we sought to describe the short-term clinical results and complications of

Table 2 MRI implant artifact scores and intraobserver reliability analysis

			Carbon fiber		Titanium control			
Read number	Sequence	Region	Mean	Range	Mean	Range	*p* value	Weighted kappa[a]
1	T1	Cortex	3.8	(2–5)	2.8	(2–3)	0.02	0.8
		CMJ	3.6	(2–5)	2.4	(2–3)	0.006	0.72
		MBI	4.3	(3–5)	2.9	(2–4)	0.005	0.59
	STIR	Cortex	3.8	(3–5)	2.8	(2–3)	0.009	0.64
		CMJ	3.6	(3–5)	2.4	(2–3)	0.003	0.62
		MBI	4.2	(3–5)	2.9	(2–3)	0.003	0.42
	Contrast-enhanced T1W FS	Cortex	3.9	(3–5)	2.7	(2–3)	0.003	0.62
		CMJ	3.5	(2–5)	2.5	(2–4)	0.02	0.65
		MBI	4.3	(3–5)	3	(3–3)	0.002	0.77
2	T1	Cortex	3.8	(2–5)	2.8	(2–3)	0.02	
		CMJ	3.6	(2–5)	2.5	(2–3)	0.008	
		MBI	4.2	(3–5)	3.3	(2–4)	0.02	
	STIR	Cortex	3.8	(3–5)	2.7	(2–4)	0.009	
		CMJ	3.5	(3–5)	2.6	(2–3)	0.01	
		MBI	3.9	(3–5)	3	(2–4)	0.03	
	Contrast-enhanced T1W FS	Cortex	3.9	(3–5)	2.8	(2–3)	0.003	
		CMJ	3.6	(3–5)	2.6	(2–4)	0.01	
		MBI	4.1	(3–5)	3.2	(3–4)	0.007	

[a] Weighted kappa values compare the consistency of scoring between readings 1 and 2

CFR-PEEK intramedullary nails, a novel long bone fixation composite material. These goals both serve to demonstrate the clinical relevance for an oncologic patient population who may require prophylactic fixation to prevent pathologic fracture following adjuvant treatment and tumor resection.

In the oncologic population, monitoring for recurrent disease can be difficult secondary to CT and MRI artifact, especially when examining areas adjacent to metal alloy implants. Metal hardware of different magnetic susceptibility can induce variable degrees of local magnetic field inhomogeneity resulting in distortion of the main magnetic field (B_0) and the RF field (B_1). Such distortion alters precessional frequencies in the adjacent tissues leading to frequency encoded and slice-selective image data, and as a result, spatial mis-mapping and image artifacts occur as signal loss, pixel pile-up and image distortion near the metal implants [4, 12]. Several techniques such as increasing read-out bandwidths, using shorter echo times and smaller voxel sizes, and view angle tilting [4, 12] have been developed or are under development to reduce such artifacts. However, these techniques may pose additional technical and logistical challenges such as long scan times, lack of frequency-selective fat-suppression sequences, large vendor-specific requirement, and incompatibility with older MRI scanners. Thus, using an implant that provides equivalent or

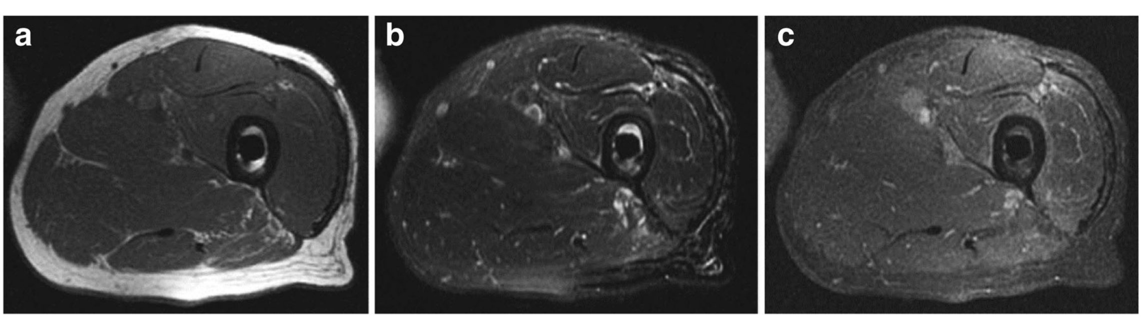

Fig. 5 MRI of a 64-year-old male with a prophylactic CFR-PEEK nail of the left femur 12 months following resection of myxofibrosarcoma in the thigh. In T1-weighted (**a**), STIR (**b**), and contrast-enhanced T1-weighted fat-saturated (**c**) sequences, the exam scored 5 in visualization of the cortex, corticomedullary junction, and muscle–bone interface. Fat suppression was considered good

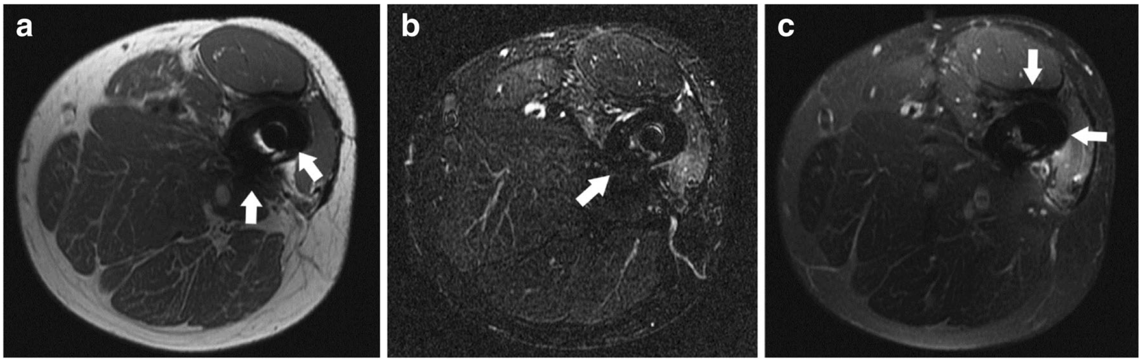

Fig. 6 MRI of a 41-year-old male with prophylactic titanium femoral nail fixation after the resection of myxoid liposarcoma in the thigh. **a** In a T1-weighted sequence, the study scored 3 in visualization of the cortex, 2 in the corticomedullary junction, and 3 in the muscle–bone interface. **b** In STIR, the study scored 3 in visualization of the cortex, corticomedullary junction, and muscle–bone interface. **c** In contrast-enhanced T1-weighted fat-saturated sequence, the study scored 2 in visualization of the cortex and corticomedullary junction, and 3 in visualization of the muscle–bone interface. Fat suppression was considered fair in STIR and poor in contrast-enhanced T1-weighted fat-saturated sequence. Focal susceptibility artifact results in the signal loss (*arrows*) in and outside of the bone near the nail

better prophylactic stabilization strength, without limitations on future imaging capabilities, argues for integrating CFR-PEEK composite implants into the oncology field. These radiographic advantages have been well documented in the spine literature where CFR-PEEK implants have been used in spine surgery for over a decade, and have also been suggested in recent trauma literature [4–7, 13, 14].

Our image analysis results clearly demonstrate an advantage of CFR-PEEK over titanium when using advanced imaging modalities of CT and MRI to examine the anatomic areas adjacent to the implant. Even with optimization of both imaging modalities, artifacts cannot completely be eliminated; therefore, there is room for development of other novel implant materials to improve the precision of current imaging technology, and possibly allow for earlier and more accurate detection of recurrent disease. However, CFR-PEEK implants likely minimize artifact sufficiently to impart a clinically significant difference on advanced imaging. This was demonstrated in our patient who developed a new femoral cortically based lesion that was clearly visualized on MRI, despite its close proximity to the CFR-PEEK nail. Larger-scale studies are needed to confirm the clinical impact of CFR-PEEK on postoperative imaging.

In our patients who received a carbon fiber nail, there were no immediate or short-term postoperative complications. The recovery milestones from surgery mirrored those of patients with titanium intramedullary nails. Implant failure was not observed, and patients returned to their preoperative functional levels, eliminating possible concerns for novel or unknown complications related to CFR-PEEK nails. Future studies with a larger patient sample size are needed to assess long-term clinical results and further evaluate the imaging benefits of CFR-PEEK.

There are several limitations in this study. Our small number of patients and MRI exams reflect the recent availability of the CarboFix nail, the low incidence of soft tissue sarcomas, and the small number of patients meeting surgical indications for prophylactic fixation with a CFR-PEEK implant. Given the variability of our patients' positions in the MRI scanners due to physical discomfort and body habitus, and the differences in their overall size, image artifact and analysis results may have been affected. This study is, however, the only known preliminary study to attempt to grade the effects of this implant in a clinical setting to the best of our knowledge, and the phantom study showed that the positioning of hardware had a substantial impact on the amount of metal artifact observed on MRI. More studies, with a larger patient cohort, are needed to evaluate the value of CFR-PEEK nails. The variable size of the bones may affect the amount of residual cortex and corticomedullary junction to be visualized on MRI given the fixed size of the nail, which requires reaming to achieve fixation in the bone. Differing surgical techniques may have introduced variable amounts of susceptibility artifact by leaving microscopic iron particles or hemorrhage, which can increase local susceptibility artifacts and may affect the visualization of tissues assessed in this study. A different radiologist may have assigned different scores depending on his or her experience due to our semi-qualitative method of grading. However, a radiologist's qualitative assessment is the current standard of clinical practice in assessing an MRI, and our MRI phantom study confirmed decreased artifact with CFR-PEEK nails.

Given the retrospective nature of this study, the imaging techniques were not the same, potentially affecting the image quality. Specifically, the orientation of the hardware could not be assessed retrospectively. Since the phantom studies demonstrated an increase in artifact with nonparallel positioning of the long axis of the hardware with respect to the *z*-axis of the magnetic field, position most certainly could have influenced scoring of images. The degree of fat saturation of the MRI studies also varied between groups, suggesting differences in

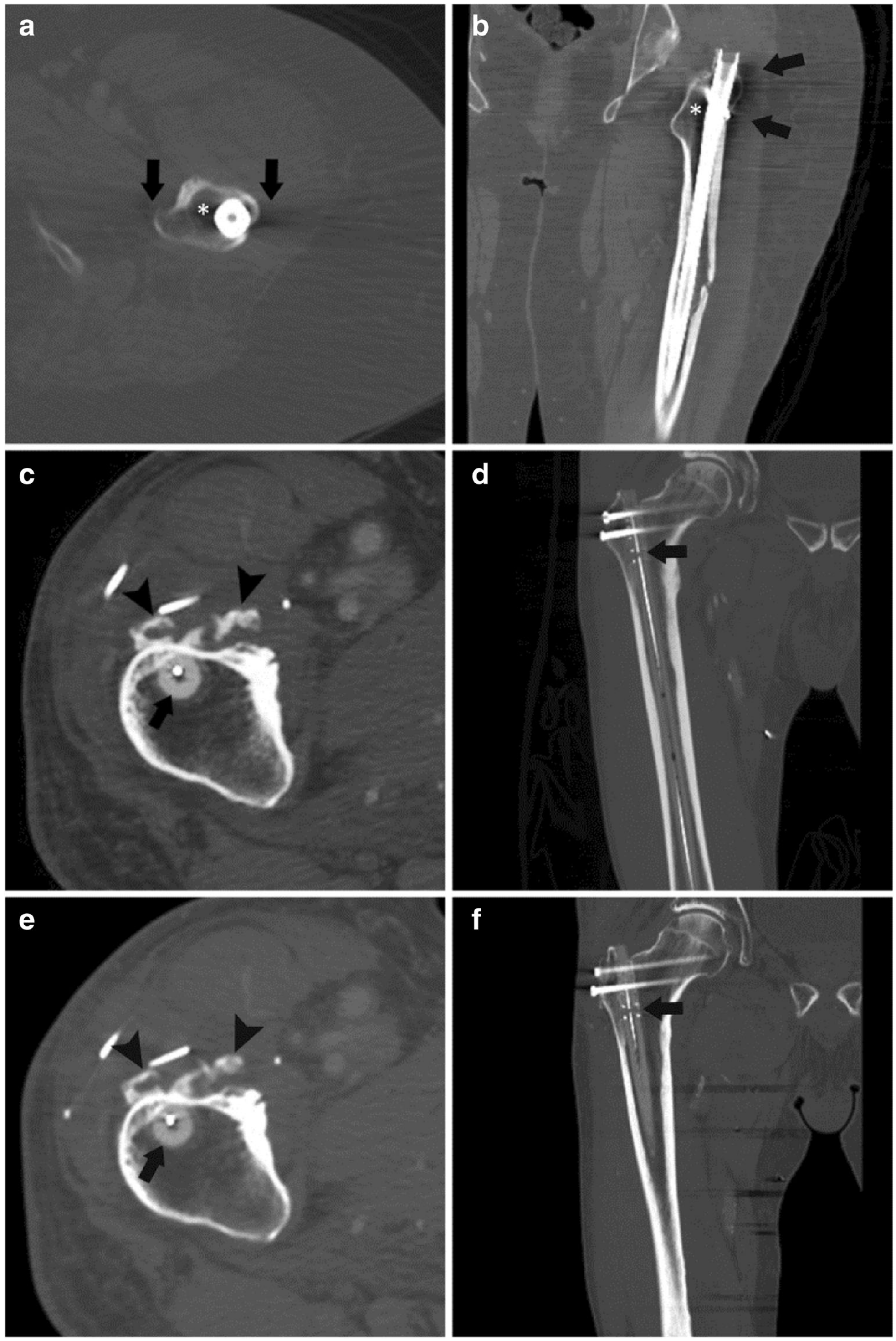

Fig. 7 A 65-year-old female with a prophylactic titanium nail placed for a pathologic fracture from metastatic breast cancer. **a** Axial and **b** coronal reformatted CT images show the beam-hardening artifacts (*arrows*) obscure the adjacent soft tissue and marrow(*). Eighty-nine-year-old male with a prophylactic CFR-PEEK nail placed after radiation and resection of a myxofibrosarcoma. **c** Axial and **d** coronal reformatted CT images show the distinct border of nail (*arrow*) within the femur and adjacent soft tissue calcifications (*arrowheads*) abutting the cortex without artifact. **e** Six-month follow-up axial and **f** coronal reformatted CT images redemonstrate a clear border of the nail (*arrow*) and adjacent soft tissue calcifications (*arrowheads*). There is no beam-hardening artifact obscuring the femur

the quality of images that may have affected scoring of the exams. This difference was minimal, however, and unlikely to have made a significant difference. Although image analysis was performed by a single radiologist, excellent intraobserver agreement, confirmed by a weighted kappa, validates the utility of this approach.

In conclusion, we believe that carbon fiber reinforced-PEEK intramedullary nail fixation is a superior alternative to titanium for patients with musculoskeletal lesions requiring prophylactic fixation and postoperative MRI or CT surveillance imaging. The clinically significant effect of CFR-PEEK nails on reducing imaging artifacts will ultimately

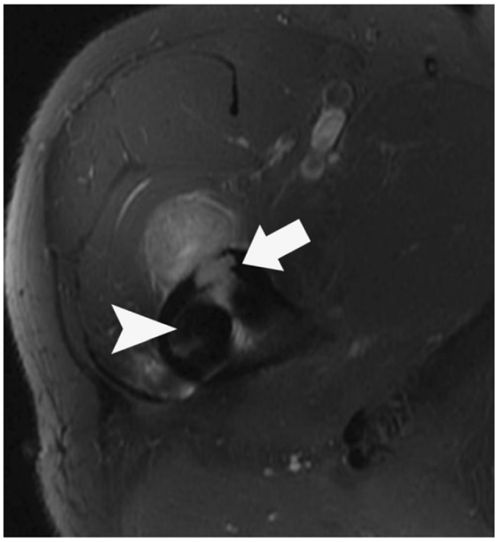

Fig. 8 Axial contrast-enhanced T1-weighted fat-saturated image of a 44-year-old man with thyroid carcinoma metastasized to the femur. The patient developed a second isolated cortically based metastasis 9 months after resection and cryosurgery of an ipsilateral femoral metastasis and placement of a CFR-PEEK nail. The metastasis (*arrow*) involving marrow and corticomedullary junction is clearly visualized immediately adjacent to the nail (*arrowhead*)

require larger studies in the future. Given the demonstrated clinical, biomechanical, and biological safety of CFR-PEEK nails, as well as the observed improvement in imaging results, the role of CFR-PEEK implants as a ideal orthopedic fixation will likely increase over time.

Acknowledgments We thank Gregory Donaldson, Yousef Mazaheri, PhD, Duane Nicholson, Bernard Woodham, and Alex Yu, all from the Department of Radiology, Memorial Sloan Kettering Cancer Center, for technical assistance with the MRI phantom imaging portion of this study. We also thank the Major Family Philanthropic Fund for its generous financial support of the Orthopaedic Fellowship Program at Memorial Sloan Kettering.

Conflict of interest The authors declare that they have no financial conflicts of interest. This study received no financial support from the manufacturer of the CFR-PEEK intramedullary nail examined.

References

1. Lin P, Schupak K, Boland P, Brennan M, Healey J. Pathologic femoral fracture after periosteal excision and radiation for the treatment of soft tissue sarcoma. Cancer. 1998;82(12):2356–65.
2. Dickie CI, Parent A, Griffin A, et al. Bone fractures following external beam radiotherapy and limb-preservation surgery for lower extremity soft tissue sarcoma: relationship to irradiated bone length, volume, tumor location and dose. Int J Radiat Oncol Biol Phys. 2009;75(4):1119–24.
3. Gortzak Y, Lockwood G, Mahendra A, et al. Prediction of pathologic fracture risk of the femur after combined modality treatment of soft tissue sarcoma of the thigh. Cancer. 2010;116(6):1553–9.
4. Koff M, Shah P, Koch K, Potter H. Quantifying image distortion of orthopedic materials in magnetic resonance imaging. J Magn Reson Imaging. 2013;38:610–8.
5. Steinberg EL, Rath E, Shlaifer A, Checkik O, Maman E, Salai M. Carbon fiber reinforced PEEK optima—a composite material biomechanical properties and wear/debris characteristics of CF-PEEK composites for orthopedic trauma implants. J Mech Behav Biomed Mater. 2013;17:221–8.
6. Kurtz SM, Devine JN. PEEK biomaterials in trauma, orthopedic, and spinal implants. Biomaterials. 2007;28(32):4845–69.
7. Baidya KP, Ramakrishna S, Rahman M. Quantitative radiographic analysis of fiber reinforced polymer composites. J Biomater Appl. 2001;15(3):279–89.
8. Sofka CM, Potter HG, Adler RS, Pavlov H. Musculoskeletal imaging update: current applications of advanced imaging techniques to evaluate the early and long-term complications of patients with orthopedic implants. HSS J. 2006;2(1):73–7.
9. White LM, Buckwalter KA. Technical considerations: CT and MR imaging in the postoperative orthopedic patient. Semin Musculoskelet Radiol. 2002;6(1):5–17.
10. Buckwalter KA, Lin C, Ford JM. Managing postoperative artifacts on computed tomography and magnetic resonance imaging. Semin Musculoskelet Radiol. 2011;15(4):309–19.
11. Takeuchi N, Hiromichi M, Tomonori N, et al. The orientation of orthopaedic metallic devices relative to the frequency-encoding gradient affects susceptibility artifacts: an experiment using open MR imaging. Fukuoka Igaku Zasshi. 2011;102(5):185–94.
12. Koch KM, Hargreaves BA, Pauly KB, Chen W, Gold GE, King KF. Magnetic resonance imaging near metal implants. J Magn Reson Imaging. 2010;32(4):773–87.
13. Collis PN, Clegg TE, Seligson D. The invisible nail: a technique report of treatment of a pathological humerus fracture with a radiolucent intramedullary nail. Injury. 2011;42(4):424–6.
14. Tarallo L, Mugnai R, Adani R, Zambianchi F, Catani F. A new volar plate made of carbon-fiber-reinforced polyetheretherketon for distal radius fracture: analysis of 40 cases. J Orthop Trauma. 2014;15(4):277–83.
15. Schwartz A, Rebecca A, Smith A, et al. Risk factors for significant wound complications following wide resection of extremity soft tissue sarcomas. Clin Orthop Relat Res. 2013;471(11):3612–7.
16. Tibbs MK. Wound healing following radiation therapy: a review. Radiother Oncol. 1997;42(2):99–106.
17. von Mehren M, Benjamin RS, Bui MM, et al. Soft tissue sarcoma, version 2.2012: featured updates to the NCCN guidelines. J Natl Compr Canc Netw. 2012;10(8):951–60.